GEOFIZIKA	Vol. 3	1986

Original scientific paper
UDC 551.524, 551.553

The dynamics of the planetary boundary layer over a heated mountain slope

Gene L. Wooldridge
Utah State University, Utah USA
and
Ernest L. McIntyre II
U. S. National Weather Service

Received 4 November 1985, in final form 5 May 1986.

The thermal structures and airflows of upslope circulations over mountain slopes were measured with temperature sondes on dualtheodolite tracked pilot and mylar superpressured balloons. Measurements were made during the developmental period of morning hours and the quasi-stationary period of early afternoon.

Upslope flows began shortly after sunrise, and quickly became deeper and stronger. By late morning, the flow field was fully established in a deep layer of a neutral atmosphere.

The potential temperature fields in vertical cross sections perpendicular to the slopes were analyzed. Data were used to calculate the solenoidal energies during periods of afternoon quasistationarity, up to heights of 800 meters above the bases of the slopes. The kinetic energies and the vertical fluxes of horizontal momentum computed for the flows over the same slopes for the same periods determined that the upward vertical fluxes reached a maximum a few hundred meters above the slope and decreased at higher elevations. The levels of upward flux divergence of horizontal momentum coincided with the levels of maximum solenoidal energy.

Dinamika planetarnog graničnog sloja iznad zagrijanog planinskog obronka

Termička struktura i strujanje zraka u cirkulaciji iznad planinskog obronka mjereni su temperaturnim sondama vezanim za pilot balone i za balone s komprimiranim plinom. Baloni su praćeni pomoću dva teodolita. Mjerenja su vršena za vrijeme razvijene planinske cirkulacije u jutarnjim satima i za kvazi–stacionarnog razdoblja rano poslije podne.

Uzlazno strujanje započinje nakon izlaza sunca i ubrzo postaje jače i zahvaća sve deblji sloj zraka. Kasno prijepodne strujno polje je potpuno razvijeno i tvori izraženi sloj neutralne atmosfere.

Polje potencijalne temperature analizirano je u vertikalnom presjeku, postavljenom okomito na obronak. Podaci mjerenja upotrebljeni su za računanje energije solenoida za vrijeme poslijepodnevnog kvazistacionarnog razdoblja do visine od 800 m iznad obronka. Kinetička energija i vertikalni turbulentni tokovi, izračunani za strujanje iznad istih obronaka i u istom vremenskom razdoblju, pokazali su da ti vertikalni tokovi dosižu maksimum nekoliko stotina metara iznad obronka, opadajući na većim visinama. Nivoi divergencije vertikalnih turbulentnih tokova poklapaju se s nivoima maksimalne energije solenoida.

1. Introduction

1. 1. Mesoscale energetics and transport processes represent critical links between microscale radiative exchanges and sensible and latent heat fluxes; they also affect mesoscale circulations. Daytime radiation absorbed by sloping terrain warms the air near the surface. This air then becomes warmer than the air in the "free" atmosphere distant from the slope, but at the same level. The turbulent transports and advection then determine the thermal structure and the available energy of the mesoscale atmosphere; the circulation is accelerated if this available energy is not balanced by momentum fluxes and dissipation. The essentially baroclinic nature of slope wind systems was established by Jeffreys (1922).

If the hydrostatic principle can be assumed, at a given height in a region influenced by slope heating, the atmospheric pressure becomes higher than at a point farther from the slope, causing air at upper levels to move away (Atkinson, 1981). Horizontal temperature differences of several degrees Kelvin are not uncommon (Buettner, 1968) over horizontal distances of a few kilometers, resulting in vertical wind speeds of 3 m s^{-1} or more and horizontal speeds of 2 m s^{-1} or more. The height of the lower wind system is typically equal to or less than the height of the ridge; anti-winds may be found above this lower wind system with an approximately equal height (Buettner and Thyer, 1966; Davidson, 1961).

1. 2 Air quality considerations during atmospheric inversion situations have increased interest in drainage slope flows during the last two or three decades; upslope winds have been less well observed, since they have not been considered critical to air quality problems. Consequently, although the behavior of up-slope winds is fundamental to comprehension of all mountain-valley wind systems, few studies concerned with this phenomen can be found in the meteorological literature.

1. 3 The upslope flow starts when the ground termperature has increased and exceeds the free air temperature at the same level, away from the slope, by a few degrees K. The depth increases rapidly once the underlying surface has warmed (Mendonca, 1969). Anti-winds for the upslope flows may be less well defined, or merged with flow at higher altitudes due to vertical fluxes of momentum. The fluxes are enhanced during daytime periods, when the atmospheric stability is decreased or is neutral.

If the airflow at higher levels, above the anti-winds, is strong enough, this vertical momentum exchange can reverse the normal slope and/or valley winds, depending to some extent on the orientation of the valley with respect to airflow aloft. That is, a turbulent shear layer forms between flows that are nearly perpendicular to each other, and the flows retain their independent directions. When flows in a valley or along a slope are within an angle of 30 degrees or so of the flow at altitude above, there is a tendency for them to merge if the wind speed aloft is sufficiently strong.

1. 4 Margules (1903) studied mesoscale energetics in and near frontal zones, where strong horizontal thermal gradients and wind shears could be easily identified. He called that portion of the internal and potential energies that could be transformed into kinetic energy the "available kinetic energy". Later, Lorenz (1955) expanded these concepts

when sufficient macroscale upper air meteorological data became available to investigate atmospheric energy generation transformation, and dissipation on a global scale. In this landmark work, he used the term "available potential energy", to denote that atmospheric energy due to thermal fields which could be transformed into kinetic energy. More recent research has applied these concepts and related the generation and transformation of potential and kinetic energies to decreasing scales of motion, until presently application is being made to the subsynoptic and meso-scales (Smith, 1969; Smith, Vincent, and Edmon, 1977, and Westbrook, 1982, among others).

1.5 In 1942, Prandtl showed that the wind speed over a slope is proportional to the potential temperature disturbances at the ground, and is independent of slope angle. He noted that, at that time, he knew of no quantitative investigations of winds at a slope.

In considering the energetics of slope winds, Thyer (1966) determined that wind strength essentially depended on the baroclinic field over the slope. He assumed hydrostatic balance and that pressure surfaces were approximately horizontal compared to temperature surfaces in baroclinic zones, and computed the available energy in the form: $\iint_A \frac{g}{\theta}\frac{\partial\theta}{\partial y}\,dA$, where g is the acceleration due to gravity, θ is the potential temperature, and y is a horizontal coordinate perpendicular to the slope.

The energy field was also measured along the axis of a mountain valley by Fosberg (1967). He found that the solenoidal field developed to a maximum strength near mid-day, and was approximately stationary until mid- to late afternoon. The location of the center of the solenoidal field was found about 500 meters above the valley floor, moving upward and upvalley during the late morning hours; maximum $\iint_A \frac{g}{\theta}\frac{\partial\theta}{\partial y}\,dA$ was calculated at about 3×10^{-5} joules kg^{-1}. The conversion of the potential energy to kinetic energy appeared to have reached a maximum during mid-day, producing a balance between energy generation, energy conversion, eddy kinetic energy, and frictional dissipation.

2. Application of the circulation theorem

V. Bjerknes' circulation theorem can be used to describe a slope breeze when written in a two-dimensional form as follows:

$$\frac{dC}{dt} = \oint \left(\frac{dv}{dt}\,dy + \frac{dw}{dt}\,dz\right) = -\oint \frac{dp}{\rho} - k_f C \tag{1}$$

where the circulation is defined as:

$$C = \oint \mathbf{V}\cdot d\mathbf{l} = \oint (v\,dy + w\,dz). \tag{2}$$

Here, $d\mathbf{l}$ is an element of length along the circulation path, K_f is a frictional drag coefficient, $\mathbf{V}$ is the wind velocity, p is the atmospheric pressure, ρ is the atmospheric density,

and v and w are the component wind velocities in the horizontal and the vertical directions, respectively.

2.2 As suggested earlier, the acceleration of the circulation is approximately zero during periods of quasi-stationarity, and the drag force $K_f C$ is nearly equal to the "driving force", $-\oint \frac{dp}{\rho}$.

This driving force can be rewritten through application of Stokes' theorem in the form:

$$-\iint_A \nabla_2 \alpha \times \nabla_2 p \cdot dA \tag{3}$$

with A equal to the cross-sectional area of the circulation cell, and α is the specific volume, defined as

$$\alpha = \frac{1}{\rho}. \tag{4}$$

When considering a circulation along a mountain slope, the Coriolis effects may be neglected, and the differences between the absolute circulation and the relative circulation, as discussed by Fleagle and Businger (1980) are quite small. The relationship (3) is sometimes referred to as the "solenoid" term (Hess, 1959). The number of solenoids N can be expressed, in two dimensions, as:

$$N_{(\rho,p)} = R_d \iint_A p^{-1} \left(\frac{\partial T}{\partial y}\frac{\partial p}{\partial z} - \frac{\partial T}{\partial z}\frac{\partial p}{\partial y}\right) dA \tag{5}$$

in which T is the temperature, and R_d is the gas constant for dry air. Under neutral conditions, usually found during midday periods above the first 100 meters over a heated slope, the horizontal pressure gradient becomes vanishingly small compared to the horizontal temperature gradients. Assuming the hydrostatic approximation, one can say that

$$\frac{\partial T}{\partial z}\frac{\partial p}{\partial y} \ll \frac{\partial T}{\partial y}\frac{\partial p}{\partial z}$$

and reduce (5) to the form used by Fosberg (1967) for circulation in two dimensions:

$$-\oint \frac{dp}{\rho} = -\iint_A \frac{g}{\theta}\frac{\partial \theta}{\partial y} dA \tag{6}$$

3. Development of an upslope flow

3.1 The initiation and development of an upslope flow was investigated in the deep, narrow Carbon Creek valley immediately west of Crested Butte, Colorado, on the morning of 3 June 1980 by the author and colleagues from Utah State University. The flows along and over the slope were detailed by a series of low-level superpressured mylar balloons. These balloons are only slightly extensible, and have a high drag coef-

ficient. As such, they tend to move along an equilibrium density level, but are sensitive to the movement of air flows, and approximate the airflow trajectories. The use of mylar superpressured balloons for determining airflow characteristics has been discussed by Cherry (1971) and Angell et al. (1972), who established that they are suitable for use as quasi-Langrangian tracers. Vertical temperature soundings were made with a portable system, using sondes mounted on 30-gram pilot balloons. All balloons were tracked with a dual-theodolite technique, providing X, Y, Z locations and u, v, and w component wind velocities at 30-second intervals.

The valley slopes down to the east. The elevation of the valley bottom is about 2850 m above mean sea level (msl) at the observation site. The valley axis is approximately west to east, and the study slope, along the northern side, had an umimpeded southerly exposure.

3.2 The horizontal (X-Y) projections and the vertical long sections (Y-Z) of four of the mylar balloon trajectories are shown in Figure 1. The mylar balloon launched from the base of the slope at 0703 Mountain Standard Time (MST) described a slow, irregular trajectory that started up the slope, subsided, and again traveled over the slope at elevations of 50 to 100 m above the surface to a point 1.5 km from the launch point after 35 minutes of flight time.

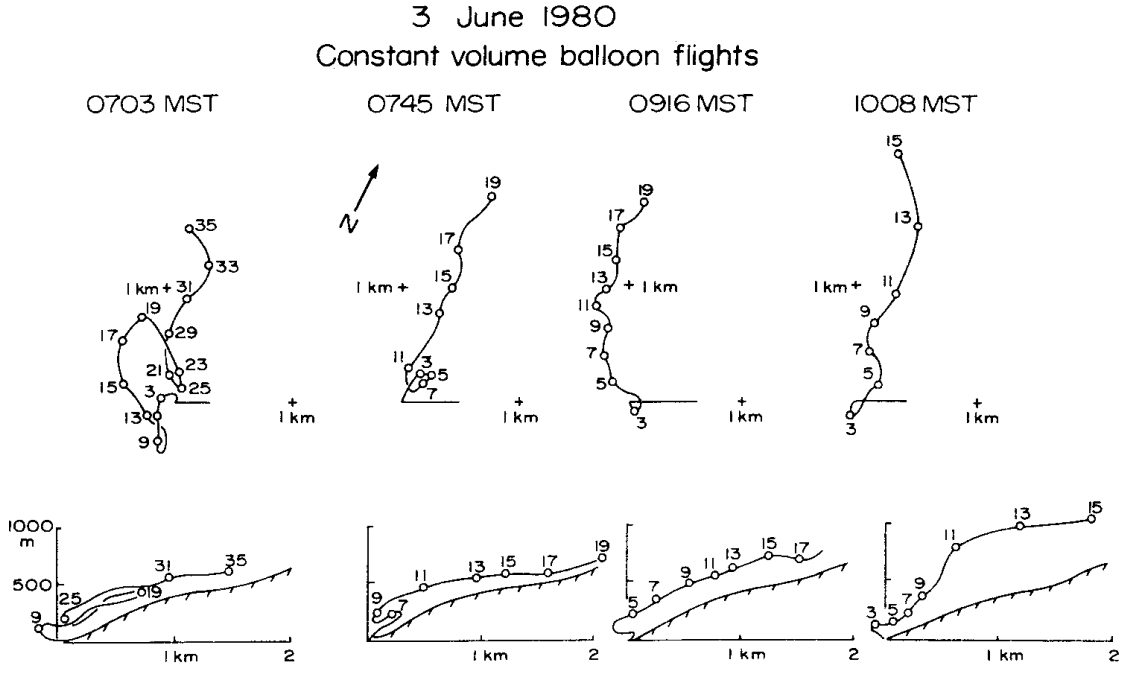

Figure 1. Trajectories of four superpressure balloon flights within Carbon Creek Valley, Crested Butte, Colorado. The upper four diagrams show projections on a horizontal plane; the lower four are projections on a vertical "long" section. Open circles are positions at given minutes after launch.

The second balloon was launched at 0748 MST. After some brief irregular motions near the base of the slope, it moved more briskly along the slope, still close to the surface, reaching a point 1.9 km from the launch point after 19 minutes of flight. The third balloon, launched at 0916 MST, showed a more uniform upslope motion, at a slightly higher elevation over the slope. By 1008 MST, the last mylar balloon of the series released spent four or five minutes in the lowest part of the valley, rose to an elevation of about 200 m above the surface, and traveled 2.2 km in 15 minutes.

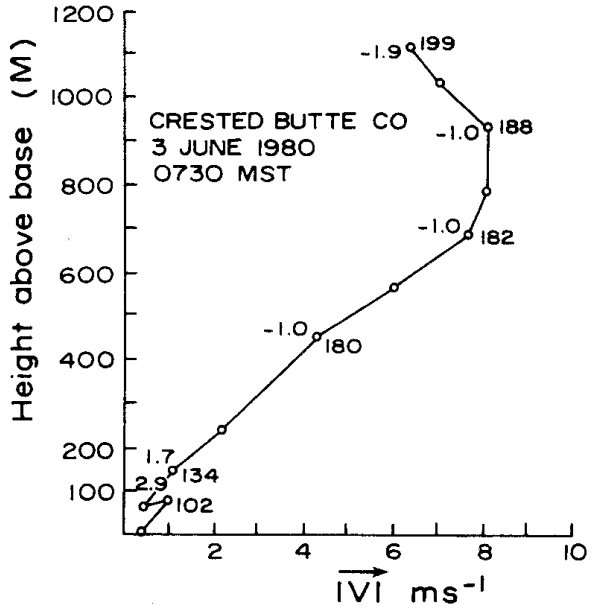

Figure 2. 0730 Mountain Standard Time sounding at Carbon Creek site, Crested Butte, Colorado. Temperatures in degrees Celsius are given to the left of the open circles; wind directions in degrees are to the right.

3.3 The 0730 MST temperature sonde showed lapse conditions to an elevation of about 150 m, capped by a deep isothermal layer. The wind direction at the valley floor was weakly upvalley, but mostly southerly above (Figure 2). By 0846 MST (see Figure 3), the lower 1000 m of the atmosphere had warmed dramatically, and a super-adiabatic layer extended to about 150 m, with a deeper neutral layer extending to the top of the sounding, 1200 m above the valley floor. The sky was clear, except for small fair-weather cumulus clouds over the mountain ridges by mid-day.

3.4 The development of the atmospheric thermal structure, and the nature of the upslope flows are demonstrated in Figures 1, 2 and 3. Over a three-hour interval ending at 1023 MST, the upslope winds had changed from an irregular motion close to the slope surface to a deeper, stronger flow regime. The maximum wind speed at about 200 m above the slope was 9 m s^{-1} as shown in the 0846 MST sounding. By the time of the second sounding, the atmosphere was neutral to a depth of at least 1200 m above ground level.

3.5 The vertical fluxes of horizontal momentum calculated from the mylar balloon trajectories were calculated as: $\overline{\rho v' w'}$, where v' is the perturbation of the horizontal velocity, w' is the perturbation of the vertical velocity, and ρ is the atmospheric density.

During the first three flights, the fluxes were upward at the mean balloon heights: for the 0703 MST flight, the flux was +0.23 N m^{-2}; for 0745 MST, +0.23 N m^{-2}; and for 0916, +0.17 N m^{-2}. These values indicate that transformation of the potential energy in the initial upslope circulation provided momentum at those levels for transport upward into the air at higher levels. By the time of the last flight (1008 MST), the flux of -0.43 N m^{-2} indicated penetration of momentum from the larger scale flow at higher levels downward into the valley.

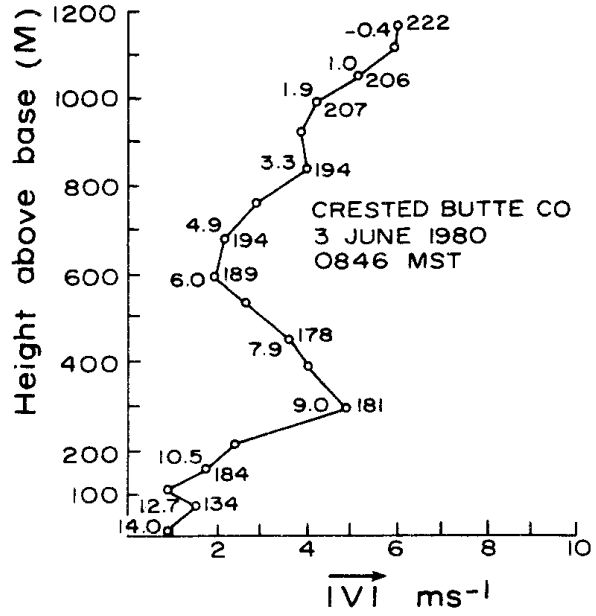

Figure 3. 0846 Mountain Standard Time sounding at Carbon Creek site, Crested Butte, Colorado. Temperatures in degrees Celsius are given to the left of the open circles; wind directions are in degrees to the right.

4. Fully-developed upslope flows

A field experiment was designed to measure the mesoscale airflow patterns and the atmospheric potential and kinetic energies over a sunlit slope during the early afternoon, when upslope winds could be expected to have reached a state of near-stationarity. The field program in Crested Butte, Colorado, and described above has since demonstrated that vertical fluxes of heat from the underlying surface in the first few hours after sunrise strongly warm the atmosphere. Thus, it appears that the condition of near-stationarity can be met before midday.

For this experiment, a mixed sequence of mylar superpressured balloons and 30-gram pilot balloons was released over a period of two to three hours. All balloons were equipped with temperature sondes, and were tracked with the dual theodolite technique. The mylar balloons travelled in quasi-horizontal trajectories, while the pilot balloons rose more nearly vertically. This provided a kind of nonorthogonal grid of temperature and wind data in a vertical section of the atmosphere over the heated mountain slope. A number of observation sites were chosen in the Cache Valley of Northern Utah (Figure 4) for this purpose, making use of both east and west slope aspects.

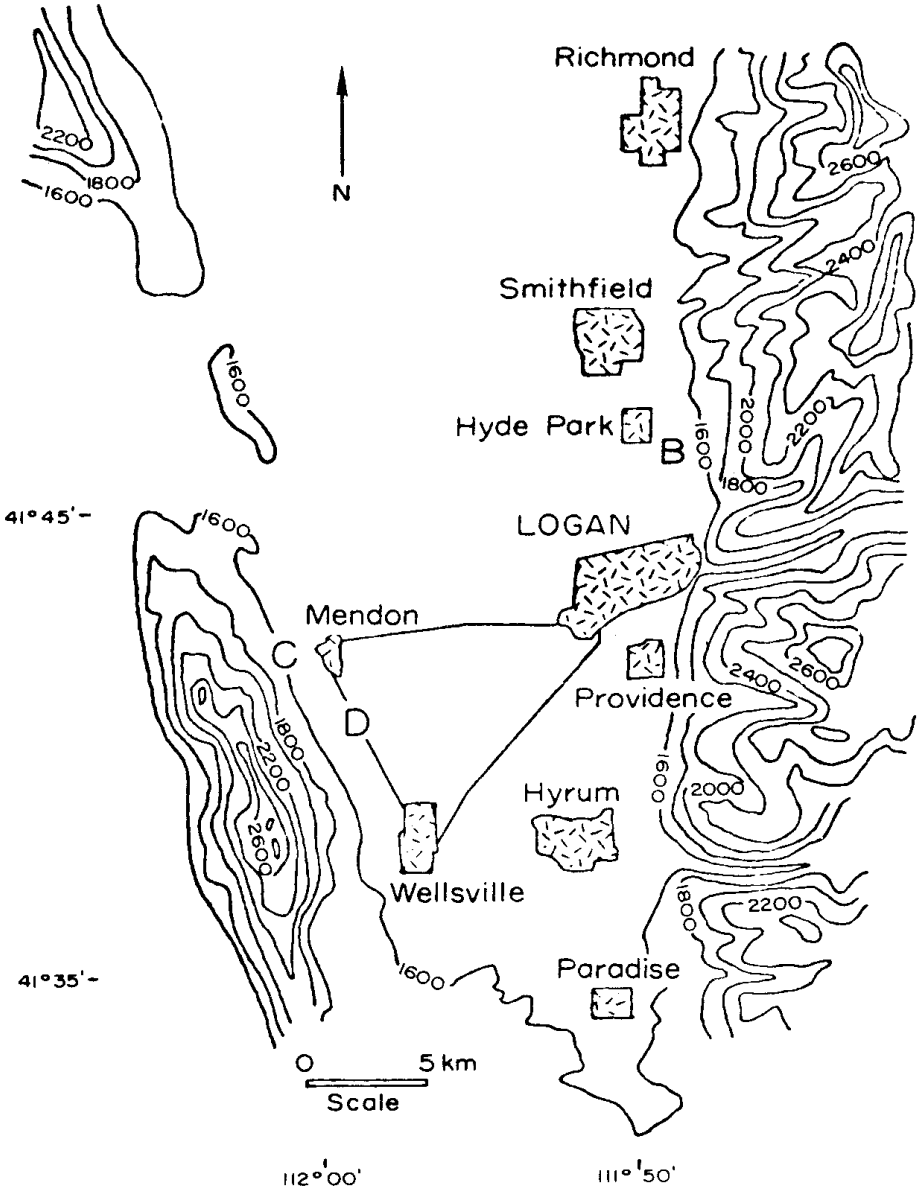

Figure 4. Contour map of Cache Valley region of northern Utah. The contours are given in meters above mean sea level, at intervals of 200 m. Latitude and longitude markers are given in the lower and left margins.

When sequential balloon flights passed through the same airspace, the temperatures reported from the sondes were compared to verify the assumed condition of stationarity; study periods when this test failed were not used to calculate atmospheric energy and vertical momentum fluxes reported here. Corrections for the buoyancy effects on the mylar balloons due to vertical displacement from their equilibrium density labels were made, but were found to affect the momentum flux results by less than 10%. The mean rise rates of the pilot balloons were subtracted from their vertical motion fields to obtain three-dimensional wind components to represent the flow field and to place the temperature data in the appropriate location.

The wind and temperature data were projected onto a vertical cross-section perpendicular to the mountain slope. In each case a portion of the cross-section was chosen for calculations of vertical momentum fluxes and the atmospheric energy fields. Two criteria determined the boundaries of the portion of the cross-section analyzed: first, the density of the wind and temperature data had to be sufficient to describe the flow and temperature structures; and second, the balloon paths had to be close to, or in a vertical plane perpendicular to the slope.

The data on the sections were interpolated onto grid points; the grids for the 11 April, 1978, and 26 May, 1978, cases (see Table 1) consisted of 250 m horizontal and 50 m vertical intervals, and for the remaining cases, 100 m horizontal and 50 m vertical intervals. Perturbations of v and w, the horizontal and vertical wind speeds, respectively, were obtained at grid points, and the vertical fluxes of horizontal momentum were computed as $\rho \overline{v' w'}$. The potential temperatures at grid points were calculated from the ambient temperature using the hypsometric and Poisson's equations. Values of the solenoidal term were computed through relation (6) subsequently at each grid point in the vertical cross-section, as were the kinetic energies.

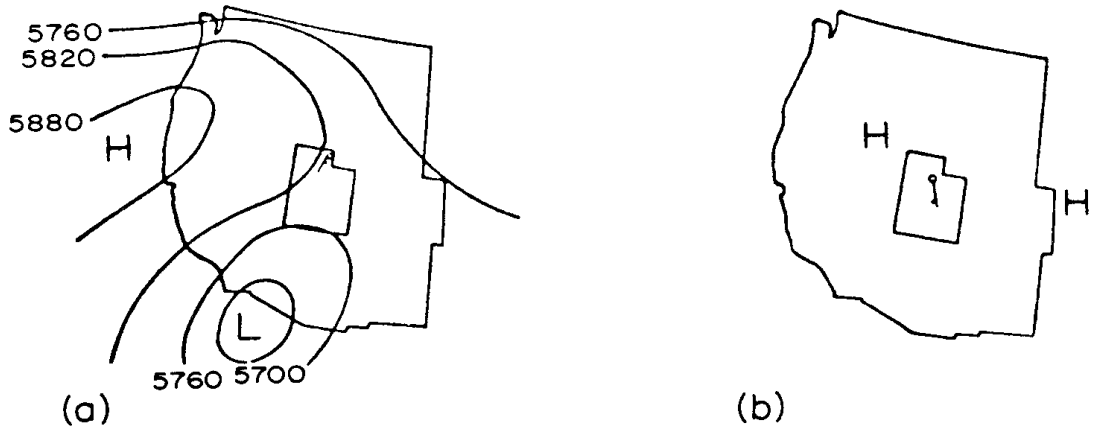

Figure 5. Essentials of the 500 mb contour chart in gpm (a), and the surface chart (b), for 0500 Mountain Standard Time, 24 October, 1978. The Salt Lake City surface wind is shown.

5. Observations of upslope flow structure

Three studies occurred over slopes with west aspects, and three over east aspects. All took place during the early afternoon under fair weather conditions. The study sites are shown as B, C, and D in Figure 4. The mountain slopes rise slowly at first, and then more sharply as the ridge lines are approached. The ridge elevations are about 1200 m above the broad, flat valley floor. Three of the six study periods are discussed briefly below.

5.1 West aspect: 24 October, 1978

Figure 5 shows the essentials of the meteorological situation for this day. The 500-mb chart indicated a weak upper level flow, while the surface wind was very weak. A high pressure center dominated the flow pattern in the lower half of the atmosphere. The sky was clear except for a few cirrus clouds, and the surface was strongly heated. Three pilot and two superpressured balloons were launched to measure the temperatures and the airflow; these data are analyzed in Figure 6.

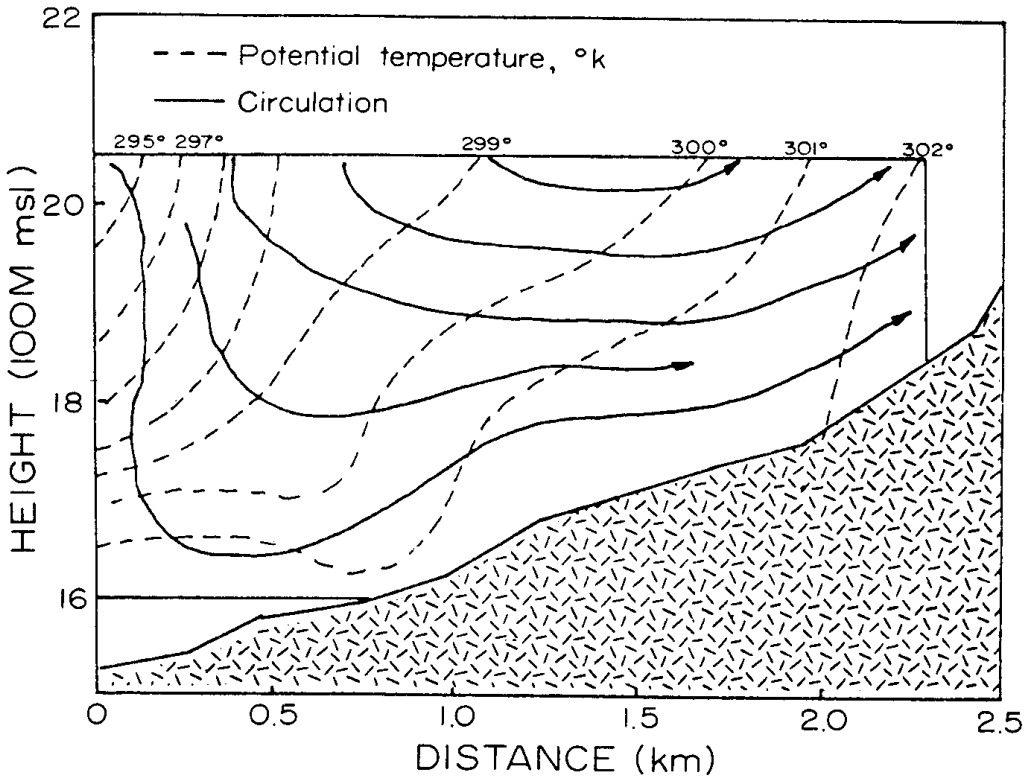

Figure 6. Airflow and potential isotherm patterns along a mountain slope in Cache Valley, Utah, on the afternoon of 24 October, 1978.

Air was descending near the base of the slope, and ascending along the slope itself. This behavior was typical of the study periods. The slope circulation was confined to the region over the slope, and did not extend over the valley floor. If balloon launches

were attempted only a few hundred meters further onto the valley floor, the balloons were entrained into the valley circulations rather than the slope circulations. These observations lend credence to the study performed earlier by Fosberg (1967), whose coordinate system used a long section of his valley, perpendicular to the sense of the coordinate system used here (see Figure 7). The potential temperature surfaces on this date sloped sharply upward instead of lying generally parallel to the terrain below.

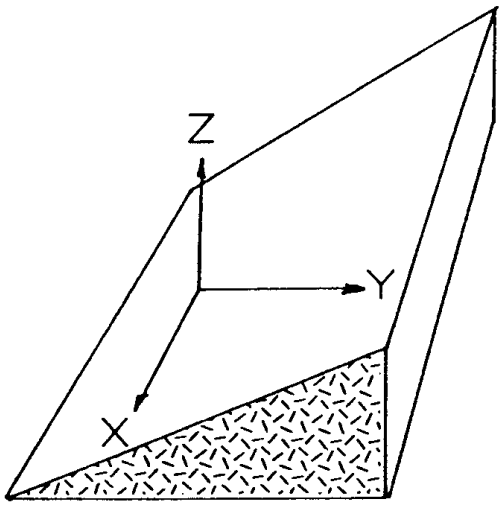

Figure 7. Geometry of the coordinate axes for calculations of relation (6) with respect to an idealized mountain slope.

5. 2 East aspect: 26 May, 1979

As indicated in Figure 8, the macroscale circulation pattern was very weak at 500 mb, and the surface wind also was weak. The surface wind at the balloon launch site was less than 2 m s^{-1}. The sky was clear except for a few fair weather cumulus clouds over the mountain ridges. Some snow remained from the previous winter at elevations greater than 800 m above the valley floor.

Two pilot and two superpressured balloon flights provided the temperature and wind data for the airflow and potential temperature fields shown in Figure 9. It can be seen that the thermal gradients were weaker than those found in the previous case, but the wind speeds were comparable. The vertical flux profile for momentum shows a deep layer of strong upward flux (Figure 10).

To compare the magnitude of the solenoidal term with the friction term (momentum divergence) term in (1), a calculation of the line integral $\oint \frac{1}{\rho}\frac{\partial \tau}{\partial z} \cdot d\mathbf{r}$ around the area revealed a value of 23.8 joules kg^{-1} for 26 May 1979 vs 28.7 joules kg^{-1} for the solenoidal term, indicating an approximate balance between these two terms.

Turbulent heat fluxes were also calculated for the 26 May case, along the upper border and at a distance of 100 m above the surface along the lower border. This heat flux was an average of 312 watts m^{-2} over the upper boundary and 232 watts m^{-2} along

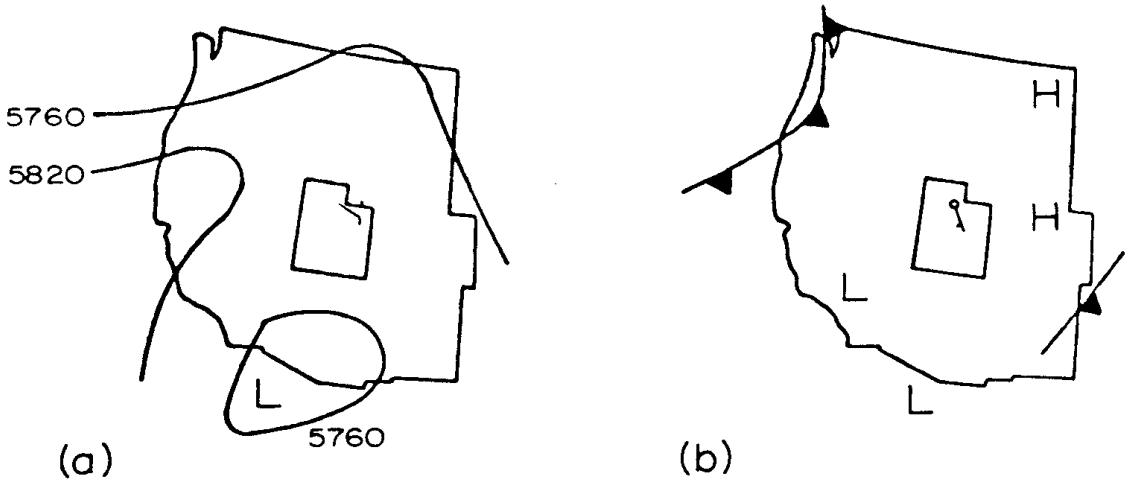

Figure 8. Essentials of the 500 mb contour chart (a), and the surface chart (b), for 0500 Mountain Standard Time, 26 May, 1979. The Salt Lake City surface wind is shown.

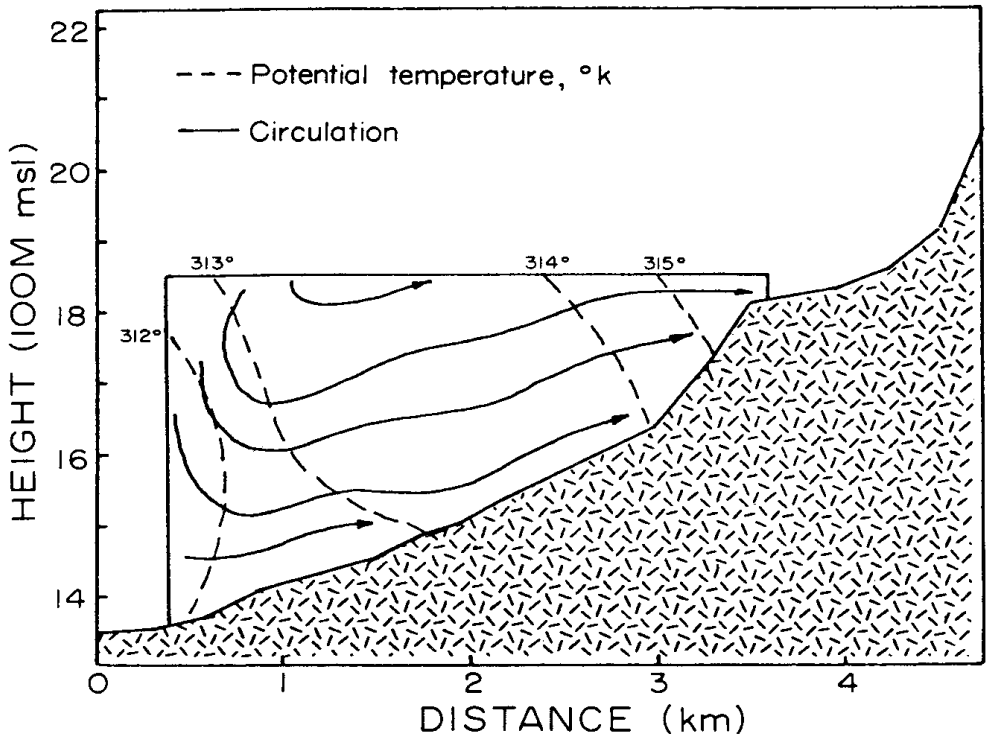

Figure 9. Airflow and potential isotherm patterns along a mountain slope in Cache Valley, Utah for the afternoon of 26 May, 1979.

the lower. Since the horizontal and vertical grid spacings for these calculations were rather coarse, the flux calculations at the lower boundary would not include fluxes due to smaller eddies close to the surface, and consequently would be expected to underestimate the vertical fluxes there.

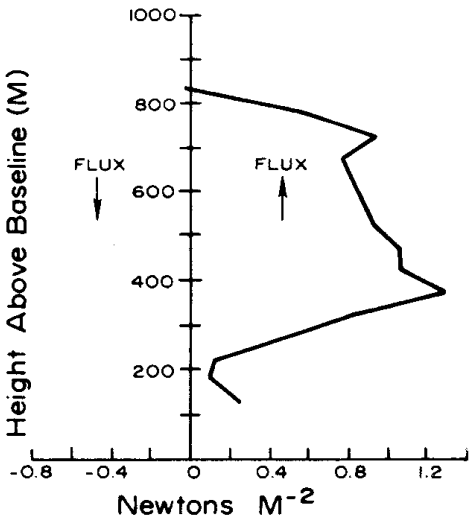

Figure 10. Vertical profile of the vertical fluxes of horizontal momentum over a Cache Valley slope for the afternoon of 26 May, 1979.

5.3 East aspect: 26 October 1978

The 500 mb circulation was moderate and from the north, but again the surface winds were light at the launch site (Figure 11). The slope was in full sunlight, but at a low angle from over the mountain ridge to the west. Two pilot and two superpressured

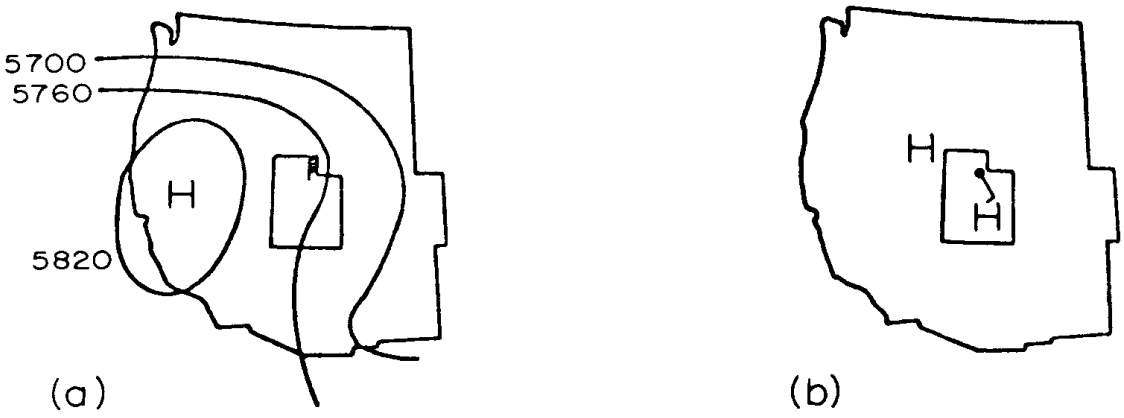

Figure 11. Essentials of the 500 mb contour chart (a) and the surface chart (b), for 0500 Mountain Standard Time, 26 October, 1978. The Salt Lake City surface wind is shown.

mylar balloons were released from near the base of the slope to sound the temperature and track the winds over the slope. The pilot balloons indicated an upslope flow depth of about 475 m, with a return, or anti-wind over the slope flow up to an altitude of about 800 m above the valley floor. A northerly gradient flow prevailed over the top of the anti-wind.

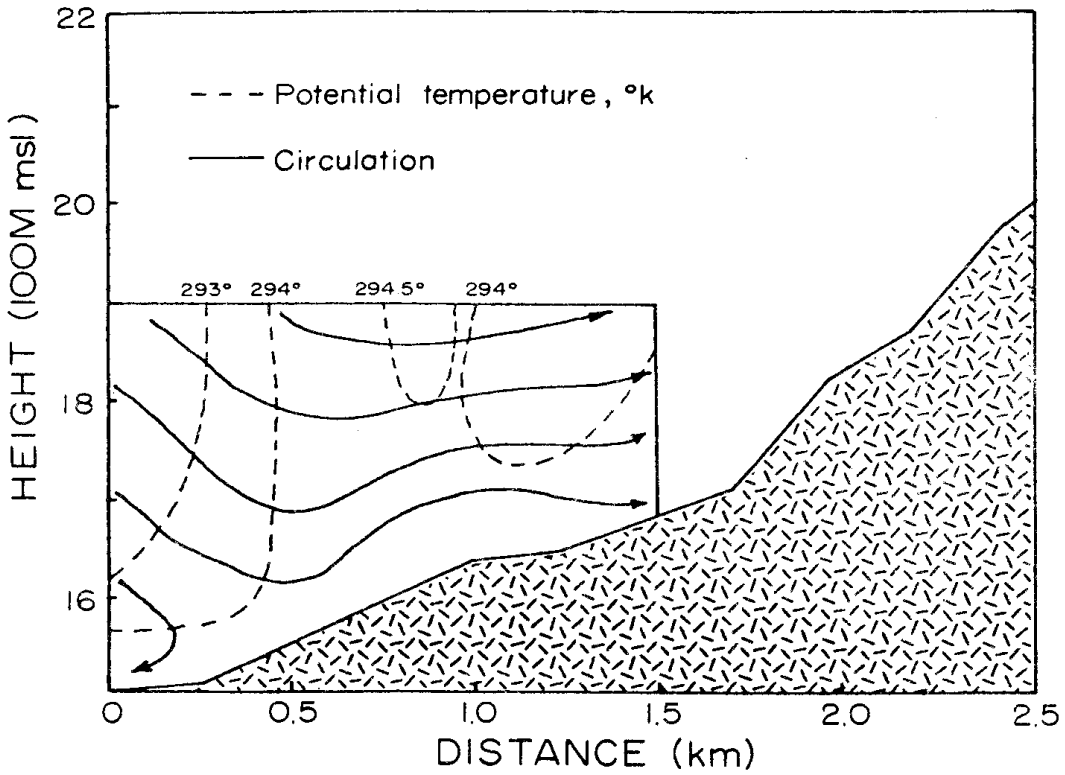

Figure 12. Airflow and potential isotherm patterns along a mountain slope in Cache Valley, Utah for the afternoon of 26 October, 1978.

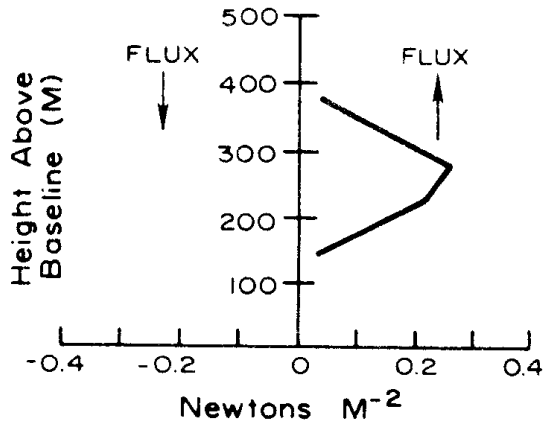

Figure 13. Vertical profile of the vertical fluxes of horizontal momentum over a Cache Valley slope on the afternoon of 26 October, 1978.

The potential temperature field (Figure 12) was weaker than on 24 October, and the horizontal thermal gradient was reversed near the slope. The circulation and the momentum fluxes (Figure 13) were weak, with upward momentum fluxes confined to the lower levels.

6. Discussion of upslope flow dynamics

6.1 The calculated solenoidal, or available potential, energy and the kinetic energy of the upslope flow regions are presented in Table 1. The energy density in joules kg^{-1} m^{-2} represents the energy per unit mass per unit area in the *Y-Z* plane of study. Integrated over the area studies, this yields joules kg^{-1}, the energy per unit mass. Some generalizations from this small sample of six experimental periods appear reasonable.

Table 1: Summary of solenoidal and kinetic energies for the upslope flow study periods

Date	joules kg^{-1} m^{-2}	joules kg^{-1}	Site	Aspect
13 Oct., 1978	$6.5 \cdot 10^{-5}$	4.6	B	West
18 Oct., 1978	$6.2 \cdot 10^{-5}$	3.4	B	West
24 Oct., 1978	$8.0 \cdot 10^{-5}$	4.9	B	West
26 Oct., 1978	$3.4 \cdot 10^{-5}$	2.7	C	East
22 May, 1979	$5.2 \cdot 10^{-5}$	1.1	D	East
26 May, 1979	$3.1 \cdot 10^{-5}$	4.7	D	East

6.2 The average solenoidal energy density for the three west aspect cases was $6.7 \cdot 10^{-5}$ joules kg^{-1} m^{-2}, with circulation acceleration in the upslope sense for these horizontal vortices. For the three east aspect cases, where the slopes were not as strongly heated in the early afternoon, the average solenoidal energy density was somewhat less: $3.9 \cdot 10^{-5}$ joules kg^{-1} m^{-2}. By comparison, the maximum solenoidal energy density computed by Fosberg (1967) for circulation along a valley axis was $4.0 \cdot 10^{-5}$ joules kg^{-1} m^{-2}.

6.3 The vertical fluxes of horizontal momentum over the sunlit mountain slopes were upward in the lowest few hundreds of meters nearest to the surface. There was an indication of a zero flux level near the top of the balloon information level, resulting in a level of momentum flux convergence. Under conditions of moderate cross-valley flow in the lee of a mountain ridge near Camp Hale, Colorado, Wooldridge and Orgill (1978) also found a flux convergence of momentum in the upper portion of a horizontal vortex.

6.4 The potential isotherms in the cross-sectional areas of the slope circulations studied here indicate that strong horizontal temperature gradients extend farther from

the slope surfaces than indicated by Orville's (1968) model of slope winds. In several cases the strongest horizontal potential temperature gradients were at 300 m to 500 m above the base of the slope, approximately as was found by Fosberg (1967), indicating that the circulations are driven by the region of the atmosphere well removed from the slope. This contrasts with the potential isotherm pattern produced by Thyer's (1966) model of slope winds, where the isotherms were oriented nearly horizontally except in a thin layer of air near the slope surface.

6.5 The average ratio of available potential energy to kinetic energy is 12.2. This compares to estimates by Oort (1964) of 3.7 and Wiin–Nilsen (1965) of 5.8 for the macro-scale, and by Westbrook (1982) of 16 for a section of the upper Rhine Valley (3 study cases). The higher ratio in valleys and along slopes is probably due to the much stronger horizontal temperature gradients on the meso-scale than those on the macro--scale.

7. Summary

7.1 Upslope flows over mountain slopes under clear skies start and develop rapidly as the depth of the heated layer of the lower atmosphere increases shortly after sunrise. The upslope flow is first intermittent, and very close to the terrain. It grows deeper and stronger during the next two or three hours. In the high elevations under strong insolation, the mixed layer becomes first superadiabatic near the surface, and then neutral to elevations in excess of 1000 m above the surface.

7.2 By midday, horizontal temperature gradients of one to three Kelvin degrees per kilometer have developed over the mountain slope. The strongest gradients for the terrain and time of the day studied here were found at 300 m to 500 m above the base of the slope, indicating that the slope circulations are driven by this region, well removed from the slope itself. The regions of the vertical crossections with the weakest solenoidal fields were also the regions of the strongest kinetic energies.

7.3 The large potential energy over the mountain slopes is due to intense horizontal temperature gradients generated by the strong afternoon insolation. These gradients are significantly greater over slopes with westerly aspects than gradients over easterly aspects at this time of day, indicating that the atmosphere responds rapidly to the heating of the terrain surface, up to several hundreds of meters above the surface.

7.4 The transformation of the available potential energy to kinetic energy of the slope flow circulations provides momentum. This momentum is transported upward by turbulent fluxes from a wind speed maximum. The height of this maximum wind speed depends on the stage of development of the circulation, and on the strength of surface heating.

Acknowledgements

This research has been supported by the United States Department of Agriculture Forest Service and the Utah State University Agricultural Experiment Station. Mrs. Eleanor Watson typed the English language manuscript. Translation from the English for this journal was graciously accomplished by Dr. Inga Lisac.

References

Angell, J. K., D. H. Pack, L. Machta, C. R. Dickson, and W. H. Hoecker (1972): Three--dimensional. air trajectories determined from tetroon flights in the planetary boundary layer of the Los Angeles Basin. Journal of Applied Meteorology, **11**, 451–471.

Atkinson, B. W. (1981): Meso-scale Atmospheric Circulations. Academic Press, London, 217.

Buettner, K. J. K. (1968): Valley wind, sea breeze, and mass fire: three cases of quasi--stationary airflow. Proceedings of the Symposium on Mountain Meteorology. Reiter, E. R., and J. L. Rasmussen, Editors. Colorado State University Atmospheric Science Paper No. 122, 103–129.

Buettner, K. J. K., and N. H. Thyer (1966): Valley winds in the Mount Ranier area. Archiv für Meteorologie, Geophysik und Bioklimatologie, B 14, 125–147.

Cherry, N. J. (1971): Characteristics and performance of three low-cost superpressure balloon (tetroon) systems. Journal of Applied Meteorology, **10**, 982–990.

Davidson, B. (1961): Local wind circulations: final report, Vol II. Studies of the field of turbulence in the lee of mountain ridges and tree lines. Contract No. DA–36––039–sc–84939, College of Engineering, Research Division, New York University.

Fleagle, R. G., and J. A. Businger (1980): An Introduction to Atmospheric Physics, 2nd Ed., Academic Press, New York, 173–176.

Fosberg, M. A. (1967): Numerical analysis of convective motions over a mountain ridge. Journal of Applied Meteorology, **6**, 889–904.

Hess, S. L. (1959): Introduction to Theoretical Meteorology. H. Holt & Co., New York, 238–243.

Jeffreys, H. (1922): On the dynamics of the wind. Quarterly Journal of the Royal Meteorological Society, **59**, 47–57.

Lorenz, E. N. (1955): Available potential energy and the maintenance of the general circulation. Tellus, 7, 157–167.

Margules, M. (1903): Über die Energie der Sturme. Jahrb. Kais–Kon Zent. für Met., Vienna. Translation by C. Abbe in Smithson. Misc. Coll, 51. (1910).

Mendonca, R. G. (1969): Local wind circulations on the slopes of Mauna Loa. Journal of Applied Meteorology, 8, 533–541.

Oort, A. H. (1964): On estimates of the atmospheric energy cycle. Monthly Weather Review, **92**, 483–493.

Orville, H. D. (1964): On mountain upslope winds. Journal of the Atmospheric Sciences, **21**, 622–633.

Prandtl, L. (1952): Essentials of Fluid Dynamics. Blackie and Son Ltd., London (translation of Prandtl, 1942), 425.

Smith, P. J. (1969): On the contribution of a limited region to the global energy budget. Tellus, **21**, 202–207.

Smith, P. J., D. G. Vincent, and H. J. Edmon, Jr. (1977): The time-dependence of reference pressures in limited-region available potential energy equations. Tellus, **29**, 476–480.

Thyer, N. H. (1966): A theoretical explanation of mountain and valley winds by a numerical method. Archiv für Meteorologie, Geophysik und Bioklimatologie, B 15, 318–347.

Wiin-Nielsen, A. (1965): Some new observational studies of energy and energy transformations in the atmosphere, in Proceedings of the Symposium of Research and Development Aspects of Long-Range Forecasting. Tech. Note No. 66, 177–202. World Meteorological Organization.

Westbrook, J. K. (1982): A study of atmospheric energetics in an open mesoscale system and the implications of anthropogenic heat and moisture on atmospheric circulations. PhD dissertation, Utah State Univ., Logan, Utah. 127 pp.

Wooldridge, G. L., and M. M. Orgill (1978): Airflow, diffusion, and momentum flux patterns in a high mountain valley. Atmospheric Environment, **12**, 803–808.

Authors' addresses: G. L. Wooldridge, Utah State University, Logan, Utah 84322–4840, U.S.A.
E. L. McIntyre II, U. S. National Weather Service